

Dynamic contrast-enhanced MRI of vascular changes induced by the VEGF-signalling inhibitor ZD4190 in human tumour xenografts

David Checkley^a, Jean J. L. Tessier^a, Stephen R. Wedge^b, Michael Dukes^b, Jane Kendrew^b, Brenda Curry^b, Brian Middleton^a, John C. Waterton^{a,*}

^aEnabling Science & Technology, AstraZeneca, Alderley Park, Macclesfield, Cheshire SK10 4TG, UK

^bCancer & Infection Research, AstraZeneca, Alderley Park, Macclesfield, Cheshire SK10 4TG, UK

Received 24 September 2002; received in revised form 25 October 2002; accepted 25 October 2002

Abstract

Dynamic contrast-enhanced magnetic resonance imaging (DCEMRI) was used to examine the acute effects of treatment with an inhibitor of vascular endothelial growth factor (VEGF) signaling. ZD4190 is an orally bioavailable inhibitor of VEGF receptor-2 (KDR) tyrosine kinase activity, which elicits broad-spectrum antitumour activity in preclinical models following chronic once-daily dosing. Nude mice, bearing established (0.5–1.0 mL volume) human prostate (PC-3), lung (Calu-6) and breast (MDA-MB-231) tumor xenografts, were dosed with ZD4190 (p.o.) using a 1 day (0 and 22 h) or 7 day (0, 24, 48, 72, 96, 120, 144, and 166 h) treatment regimen. DCEMRI was employed 2 h after the last dose of ZD4190, using the contrast agent gadopentetate dimeglumine. Dynamic data were fit to a compartmental model to obtain voxelwise K^{trans} , the transfer constant for gadopentetate into the tumor. K^{trans} was averaged over the entire tumor, and a multi-threshold histogram analysis was also employed to account for tumor heterogeneity. Reductions in K^{trans} reflect reductions in flow, in endothelial surface area, and/or in vascular permeability. A vascular input function was obtained for each mouse simultaneously with the tumor DCEMRI data. ZD4190 treatment produced a dose-dependent (12.5–100 mg.kg⁻¹ per dose) reduction in K^{trans} in PC-3 prostate tumors. At 100 mg.kg⁻¹, the largest concentration examined, ZD4190 reduced K^{trans} in PC-3 tumors by 31% following 2 doses (1 day treatment regimen; $p < 0.001$) and by 53% following 8 doses (7 day regimen; $p < 0.001$). Comparative studies in the three models using a showed similar reductions in K^{trans} for the lung and breast tumors using the histogram analysis, although the statistical significance was lost when K^{trans} was averaged over the entire tumor. Collectively these studies suggest that DCEMRI using gadopentetate may have potential clinically, for monitoring inhibition of VEGF signaling in solid tumors. © 2003 Elsevier Inc. All rights reserved.

Keywords: Dynamic MRI; K^{trans} ; Angiogenesis; VEGF signaling; ZD4190

1. Introduction

The induction of new blood vessels from an existing host vasculature (angiogenesis) is essential for supporting the growth of solid tumors [1]. Vascular endothelial growth factor (VEGF) is a key stimulus for angiogenesis, is released predominantly by tumor cells, and induces vessel sprouting by promoting endothelial cell proliferation and migration [2,3]. VEGF may also contribute to tumor growth and metastasis through its profound permeabilizing effect on the tumor vasculature. It is estimated that VEGF is

50,000-fold more potent at increasing microvessel permeability than histamine [4]. Leaky tumor endothelia enable enhanced nutrient and catabolite exchange and may provide less of a barrier to the intravasation of tumor cells. These phenotypic responses are induced following VEGF binding to the high-affinity receptors Flt-1 (VEGFR-1) and KDR (VEGFR-2) on endothelial cells. VEGF binding induces receptor homo- or heterodimerisation and the activation of intrinsic receptor tyrosine kinase activity, which is required for propagation of an intracellular signaling response. Experiments with selective agonists of Flt-1 and KDR suggest activation of KDR alone is sufficient to induce angiogenic and permeability responses to VEGF [5,6].

Disruption of VEGF-signaling inhibits angiogenesis and reduces the high vascular permeability found in tumors [7],

* Corresponding author. Tel.: +44(0)1625-513633; fax: +44(0)1625-514463.

E-mail address: john.waterton@astrazeneca.com (J.C. Waterton).

and there is evidence to support the efficacy of this approach as an anticancer strategy [8]. ZD4190 is a heteroaromatic-substituted anilinoquinazoline, which is a potent inhibitor of KDR tyrosine kinase activity and VEGF-stimulated endothelial cell proliferation *in vitro* [9]. As chronic dosing of a VEGF inhibitor may be required to prevent tumor growth, ZD4190 was designed to be active orally. Once-daily, chronic oral administration of ZD4190 (12.5–100 mg/kg/day) has been shown to inhibit the growth of histologically distinct human tumor xenografts (breast, colon, lung, ovarian, prostate) in athymic mice [9].

Examining the pharmacology of new angiogenesis inhibitors in Phase I/IIa clinical trials may require a different approach than used in traditional anticancer drug development, particularly since sustained dose administration is likely to be required, and the anticipated therapeutic outcome is prolonged stabilization of disease (increase in median survival or time to progression). There is, therefore, a recognized need for biologic markers that can be used to assess the activity of angiogenesis inhibitors at an earlier stage of treatment [10,11].

Dynamic contrast enhanced MRI (DCEMRI) has potential for assessing the biologic effect of angiogenesis inhibitors because analysis of changes in enhancement with time yields parameters that can reflect microvessel density [12] and blood flow [13,14]. This methodology can be used to detect changes in vascular permeability [15], a further parameter that may be particularly amenable to the evaluation of VEGF signaling inhibitors. Large macromolecular contrast agents are particularly effective in animal models for quantifying a reduction in vascular permeability induced by antiVEGF therapy [16], but are not generally available for clinical use. The smaller molecule gadopentetate dimeglumine, however, is a well-established agent for clinical MRI applications and has been widely used to examine tumor vascular permeability both in humans [17,18] and in animal models [19,20]. The volume transfer constant for gadopentetate between blood plasma and the extravascular extracellular space, K^{trans} , may reflect acute changes in tumor vascular permeability [21–25]. Although this parameter can be derived using a range of compartmental models, the Tofts and Kermode method [24] has been most widely employed with gadopentetate in both humans and animal models.

This study aimed to develop and deploy an MRI protocol for measuring the acute effects of VEGF signaling inhibitors. As the ultimate goal was to make the method available for use in humans, the contrast agent selected was the clinically applicable gadopentetate. Experiments were designed to examine whether DCEMRI could detect changes in K^{trans} using the Tofts and Kermode method, following acute (1 day) and short-term (7-days) administration of ZD4190 to nude mice bearing human prostate, lung and breast tumors.

2. Methods

2.1. Prostate, lung and breast human tumor xenograft models

The methods used in establishing tumor xenografts have been described in detail elsewhere [9]. Briefly, PC-3 prostate adenocarcinoma, Calu-6 lung carcinoma and MDA-MB-231 breast adenocarcinoma were established in female Swiss athymic mice by subcutaneous (s.c.) injection of 10^6 (PC-3, Calu-6) or 10^7 (MDA-MB-231) cells in the hind flank. Tumor volumes were assessed by bilateral Vernier caliper measurement, and mice bearing tumors with a volume of 0.5–1.0 mL were selected for imaging experiments.

2.2. Experimental protocol

Six separate experiments were undertaken in full compliance with the United Kingdom Animals (Scientific Procedures) 1986 Act. ZD4190 was suspended in a 1% (v/v) solution of polyoxyethylene sorbitan mono-oleate in deionized water and administered by oral gavage (0.1 mL/10 g body weight). In each experiment, mice were randomized to receive either vehicle or ZD4190, administered once daily using a 1 day (at 0 and 22 h) or 7 day (at 0, 24, 48, 72, 96, 120, 144, and 166 h) treatment regimen (i.e., daily administration of compound for 1 or 7 days with an additional dose given 2 h prior to the end of the treatment period) followed by DCEMRI under terminal anesthesia.

Each experiment included a control group that received vehicle only, and one or more groups treated with ZD4190 (12.5, 25, 50 or 100 mg.kg⁻¹ per dose). Four of the six experiments involved PC-3 tumors and for convenience of presentation, data for vehicle-treated PC-3 tumors were combined, as were data from PC-3 tumors treated with ZD4190 at 100 mg.kg⁻¹, using the 1 day treatment regimen. Animals were excluded from the analysis if they failed to complete the protocol for any reason, if the vascular input function (VIF) was not obtained, or if VIF failed to exhibit a monotonic decline after the initial peak.

2.3. MRI protocol

Animals were anesthetized with 1–1.5% halothane (Fluothane, AstraZeneca, Macclesfield, UK) for approximately three hours and mounted in a purpose-built, lidded, plastic cradle fitted with a thermocouple and electrocardiogram electrodes. Under a flow of warm air, a heparinized 26-gauge catheter was inserted into the tail vein and attached to a syringe containing 10 μ l. (g mouse weight)⁻¹ of 30 mM gadopentetate dimeglumine (Magnevist, Schering, Berlin, Germany) in sterile water. The mice were then transferred, in the cradle, to the bore of a horizontal magnet where their temperature was maintained at 38° C by a flow of warm air, and their heart rates were monitored.

2.4. Imaging acquisition protocols

Imaging was carried out using a spectrometer operating at 200 MHz (Inova, Varian, Palo Alto, CA USA), a 400 mm diameter horizontal bore 4.7T magnet equipped with room temperature shim coils and 155 mm bore gradient coils (Oxford Instruments, Oxford, UK) providing gradients up to 200 mT.m⁻¹, and a 63 mm bore quadrature birdcage transmitter receiver coil (Varian). In order to identify tumor perimeters, an initial heavily T₂-weighted multi-slice fast spin echo (FSE) sequence was carried out (repetition time TR = 3000 ms, effective echo time = 120 ms) with five slices through the tumor (voxel dimensions 0.63 × 0.31 × 2 mm). This was followed by two transverse T₁-weighted images through the abdominal aorta and vena cava, caudal to the kidneys and cranial to the femoral bifurcation, with and without a sagittal saturation slab through the heart and great vessels (TR = 500 ms; TE = 10 ms, voxel dimensions 0.23 × 0.16 × 5 mm). These two images were used to select voxels within the blood vessels in order to calculate the VIF.

A saturation-recovery sequence, consisting of four multi-slice spin-echo images (TR = 120, 500, 2000 and 10000 msec; TE = 10 ms), was then performed for T₁ mapping. Six slices were acquired: five sagittal slices through the tumor (voxel dimensions 0.63 × 0.31 × 2 mm), and one transverse through the descending abdominal aorta and vena cava (voxel dimensions 0.23 × 0.16 × 5 mm). Each line of k-space was acquired for all six slices within a single TR period; the location of the tumor on the flank ensured that the analyzed data were not affected by cross talk between the sagittal and transverse slices. No saturation band was applied in the acquisition of these data.

Finally, the dynamic run was initiated with repetitions at 16 sec intervals in a multi-slice T₁-weighted spin echo sequence (TR = 120 msec, TE = 10 msec, voxel dimensions 0.63 × 0.31 × 2 mm). Each run included five sagittal slices through the entire tumor volume (voxel dimensions 0.63 × 0.31 × 2 mm), one 4 mm sagittal saturation slab through the aorta and vena cava, and one transverse slice through the abdominal aorta and vena cava (voxel dimensions 0.23 × 0.16 × 5 mm). After five pre-contrast repetitions, gadopentetate was injected manually over 3 sec into the mouse tail-vein. This occurred 60 min after the induction of anesthesia. The dynamic run continued with repetitions every 16 sec for 53 min after the injection, providing 200 image sets.

2.5. Vascular input function

A calibration curve was obtained by measuring the T₁ relaxation times of filtered mouse blood plasma solutions containing between 0 and 1.8 mM gadopentetate. The curve was used to calculate \mathfrak{R} , the relaxivity, or increase in relaxation rate of filtered plasma per unit concentration of gadopentetate. The gadopentetate-containing plasma solu-

tions were imaged at 38° C using a saturation-recovery spin echo imaging protocol.

The voxels within the abdominal aorta and vena cava were identified as high-signal on the transverse pre-injection T₁-weighted scans acquired without the sagittal saturation slab, but low-signal following saturation. Following gadopentetate injection, the longitudinal relaxation rate ($R_1 \equiv T_1^{-1}$) of the spins within the artery and vein increased, and the signal enhancement $S_t^{blood} - S_0^{blood}$ blood increased in a relationship dependent on the concentration of contrast agent in the blood plasma:

$$[Gd]_t^{plasma} = \frac{-T_{sat}^{-1} \ln \left(\frac{S_t^{blood} - S_0^{blood}}{M_\infty^{blood}} + \exp(-T_{sat} R_{1,0}^{blood}) \right) - R_{1,0}^{blood}}{\mathfrak{R}(1-h)}$$

where $[Gd]_t^{plasma}$ (mM) is the gadopentetate concentration in the plasma at time t ; $h = 0.44$ is the mouse hematocrit [26], $R_{1,0}^{blood} = 0.4 \text{ s}^{-1}$ is the longitudinal relaxation rate of filtered mouse plasma; $\mathfrak{R} = 3.8 \text{ s}^{-1} \text{ mM}^{-1}$ calculated as described above; $T_{sat} = 75 \text{ ms}$ is the recovery time between imposition of the saturation band, and acquisition of the vessel image; M_∞ (relative units) is the equilibrium magnetisation in the vessel lumen; S_0^{blood} (relative units) is the mean vessel lumen signal from the five pre-injection scans; and S_t^{blood} (relative units) is the vessel lumen signal at time t .

Flow within the large abdominal blood vessels rapidly replaced all the saturated spins in the transverse slice. Consequently the plasma M_∞ was obtained from the T₁-weighted scan with a TR = 500 ms, a sufficiently short time to saturate non-flowing spins, but long enough for all moving spins to be replaced within the slice. The time-dependent plasma concentration of gadopentetate obtained from these calculations, was fitted to a bi-exponential decay function, representing the VIF, using a Levenberg-Marquardt algorithm:

$$[Gd]_t^{plasma} = D[a_1 \exp(-m_1 t) + a_2 \exp(-m_2 t)]$$

where $D = 0.3 \text{ mmol.kg}^{-1}$, the bolus dose of gadopentetate; the terms a_1 and m_1 represent the equilibration of gadopentetate between plasma and extracellular space a_2 and m_2 reflect the kidney clearance of gadopentetate; and $(a_1 + a_2)^{-1} \text{ l.kg}^{-1}$ represents the plasma volume of the mouse per unit body weight. This model, of Tofts and Kermode, assumes that the contrast agent is mixed instantly in the plasma, a reasonable assumption in mice given the very short blood circulation time and long injection time.

2.6. Image processing and analysis

The DCEMRI data were analyzed voxelwise using the pharmacokinetic model of Tofts and Kermode [24] to obtain the volume transfer constant for gadopentetate between blood plasma and the extravascular extracellular space

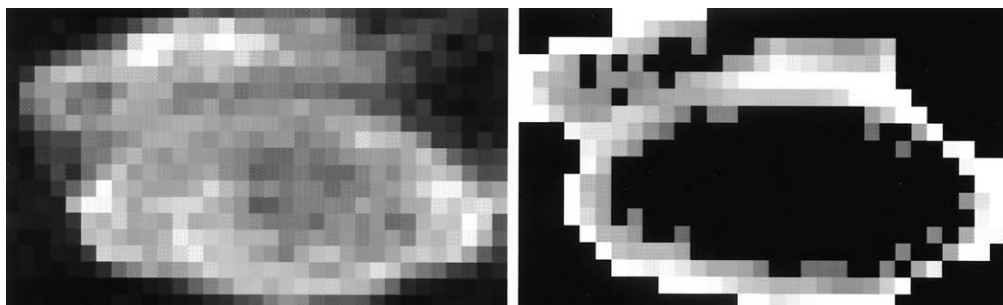


Fig. 1. Left, a T_2 -weighted image from a Calu-6 tumor following dosing with ZD4190 (100 mg/kg/dose; 7 day treatment-regimen). Only the tumor is seen in the image. Right, the equivalent K^{trans} map for the same tumor. The black central area is a region of unfitted voxels, which was often large following treatment.

($K^{trans} \text{ sec}^{-1}$), and the volume of the extravascular extracellular space (V_e). First, a region of interest (ROI), comprising the entire tumor volume, was defined using manual segmentation of the heavily T_2 -weighted FSE images. Next, the pre-contrast relaxation rate for each tumor voxel was obtained from the saturation-recovery experiment and the gadopentetate concentration in each voxel was obtained as:

$$[Gd]_t = \frac{-TR^{-1} \ln\left(\frac{S_t - S_0}{M_\infty} + \exp(-TR R_{1,0})\right) - R_{1,0}}{\mathfrak{R}}$$

where $[Gd]_t$ (mM) is the average gadopentetate concentration in the voxel at time t ; $R_{1,0}$ is the pre-contrast voxel longitudinal relaxation rate and M_∞ the equilibrium magnetisation in the voxel, both obtained from the saturation-recovery experiment; $\mathfrak{R} = 3.8 \text{ s}^{-1} \text{ mM}^{-1}$ calculated as described above and assumed to be same as in plasma; $TR = 120 \text{ ms}$; S_0 (relative units) is the mean voxel signal from the five pre-injection scans; and S_t (relative units) is the voxel signal at time t . Finally, using the time constants m_1 and m_2 characterizing the VIF for each mouse, each individual tumor voxel was fitted to the model of Tofts and Kermode using least squares parameter estimation to provide K^{trans} and V_e maps across the tumor. According to the model, after injection of a bolus dose $D \text{ mmol.kg}^{-1}$ given at time $t = 0$, the tissue concentration of contrast medium is:

$$[Gd]_t = D \cdot K^{trans} \sum_{i=1,2} \frac{\exp(-K^{trans}t/V_e) + \exp(-m_i t)}{m_i - K^{trans}/V_e}$$

Unfitted voxels comprised those where the Levenberg-Marquardt algorithm did not converge, and physiologically unreasonable values (i.e., $K^{trans} < 0$, $K^{trans} > 0.01 \text{ s}^{-1}$, $V_e < 0$, $V_e > 1$). Unfitted voxels were normally in the center of the tumor and probably resulted from a poor vascular supply in hypoxic or necrotic areas. On the basis of their very low perfusion, the unfitted voxels were included in the K^{trans} maps as zeros, and therefore contributed in calculation of tumor mean K^{trans} , but were excluded from the V_e maps.

2.7. Statistical analyses

DCEMRI data acquisition, analysis and exclusion were performed blinded as to treatment. As the group inter-animal SDs were proportional to the group means, the data were log-transformed. For the dose-ranging studies, the SD for K^{trans} in the vehicle-treated animals was 0.18 log units, which provided 90% power to detect a 35% reduction in K^{trans} . A paired t test was used to compare caliper volumes pre and post dosing. Comparisons of K^{trans} and tumor volume were made with a one tailed t test, but all other comparisons were two tailed.

As well as comparing the mean values for the whole tumors in control and treated groups, a histogram analysis was applied to the K^{trans} data. In the histogram analysis, the number of fitted voxels over a given threshold was counted for each animal in both the treated and control groups. The difference in the number of voxels per animal over a given threshold between the two groups was examined for statistical significance using a permutation test [27]. The process was repeated for a series of thresholds corresponding to accumulative 2% increments (i.e., the top 2%, 4%, 6% . . . to 100%) of the total number of voxels in both groups (obtained by pooling control or treated data), until all the fitted voxels were included. The probability value for the control group having more voxels over a given K^{trans} threshold than the treated group was then plotted against each threshold value.

3. Results

3.1. Qualitative findings

A total of 296 mice were imaged, but after imposition of exclusion criteria 187 remained for analysis. Fig. 1 shows a T_2 -weighted FSE image through a tumor. It proved possible from these images to define a ROI including the tumor, but excluding the skin. Following injection of gadopentetate, rapid signal enhancement was observed in T_1 -weighted images in the peripheral (rim) regions of the tumor. In the

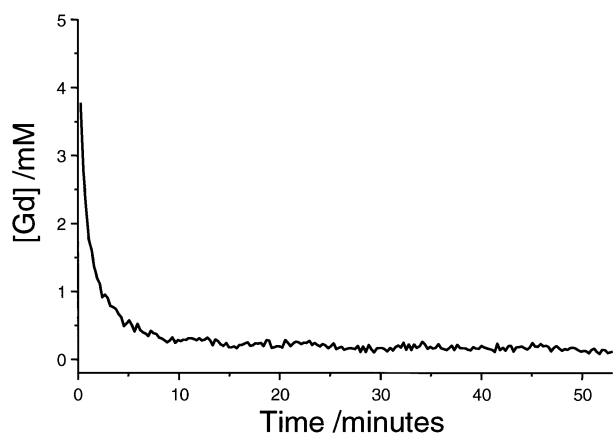


Fig. 2. Vascular input function for a single mouse, measured from the DCEMRI data in the abdominal aorta and inferior vena cava.

central regions of the tumor, signal enhancement was slower, and in some central areas, signal was still increasing when collection of the DCEMRI data finished 53 min post-injection.

3.2. Tumor volumes

The overall mean \pm SD of all pre-treatment tumors measured was 0.77 ± 0.28 mL. There was no significant inhibition of tumor growth as a result of 24-h dosing with ZD4190. However, in comparison with controls, 1-week of dosing significantly reduced tumor volume by 11% ($p = 0.035$), 13% ($p = 0.26$), and 29% ($p = 0.004$) for the prostate, lung and breast tumors, respectively. Similar effects on tumor growth have been described previously [9].

3.3. Vascular input function

Fig. 2 shows the changes in the concentration of gadopentetate in the aorta and vena cava of one animal over the time of the dynamic study, i.e., the VIF. The parameters obtained from a bi-exponential fit to the data from untreated animals were: $a_1 = 11.95 \pm 6.7$ (mean \pm SD), $a_2 = 4.67 \pm 2.08$ kg.l⁻¹, $m_1 = 0.0195 \pm 0.012$ and $m_2 = 0.0009 \pm 0.0004$ sec⁻¹. This implies a blood volume of 107 ml.kg⁻¹ (given a 44% hematocrit). In each experiment, no significant difference between ZD4190-treated and untreated animals was evident for any of the four VIF parameters measured.

3.4. Fitting the dynamic data to the compartmental model

Fig. 1 shows a typical K^{trans} map for a tumor. Rapid contrast enhancement was observed for the peripheral regions of the tumor. These voxels exhibited a fast initial rise followed by a fast decay and were characterized by high K^{trans} and V_e values (typically for the rim: $K^{trans} = 0.003$ s⁻¹, $V_e = 0.35$; for the whole tumor: mean $K^{trans} = 0.001$ s⁻¹, $V_e = 0.20$). The values of K^{trans} decreased gradually

Table 1
The effect of acute administration of ZD4190 (1 day regimen) on the K^{trans} and V_e of prostate tumours

No. of mice	Dose (mg.kg ⁻¹) ^a	K^{trans} (s ⁻¹)	V_e
45	0	0.00098 ± 0.00045	0.22 ± 0.092^b
9	12.5	0.00078 ± 0.00034	0.17 ± 0.051
10	25	0.00099 ± 0.00050	0.21 ± 0.082
7	50	0.00089 ± 0.00031	0.27 ± 0.089
32	100	0.00067 ± 0.00027	0.18 ± 0.052

^a Two doses of ZD4190 were given to mice 24 hour and 2 hour prior to DCEMRI.

^b Values are mean \pm SD.

100 mg/kg shows significant K^{trans} reduction ($P < 0.001$) but no significant effect was detected at the lower doses.

from the periphery to the center of the tumor. In the center of the tumor, voxels were often unfittable; where fittable, K^{trans} was usually low, although both low and high values of V_e were observed. The majority of voxels could be fitted to the compartmental model used. However, one week of treatment with daily doses of 100 mg.kg⁻¹ ZD4190 significantly increased the percentage of unfitted voxels in the breast (34% when treated cf. 18% when untreated, $p = 0.003$), lung (37% cf. 24%, $p = 0.03$) and prostate (35% cf. 11%, $p < 0.001$) tumors. The percentage of unfitted voxels was also increased following 24-h dosing in the breast (27% cf. 18%, $p = 0.06$) and lung (33% cf. 24%, $p = 0.03$) but not the prostate (12% cf. 11%, $p = 0.2$) tumors.

3.5. Dose-ranging studies in the prostate tumors

Table 1 summarizes the results of the dose-ranging experiments in the human prostate tumor model studied. Twenty-four hour dosing with 100 mg.kg⁻¹ ZD4190 led to a highly significant 31% reduction in K^{trans} ($p < 0.001$) and a significant reduction in V_e (22% $p = 0.01$). There was a trend for a dose-dependent reduction in K^{trans} ($r = -0.72$), but there was no dose response relationship for V_e .

3.6. Comparative studies in prostate, lung and breast tumors

In view of the highly significant effects seen with a 100 mg.kg⁻¹ dose of ZD4190, this dose was selected for subsequent comparative studies in prostate, lung, and breast tumors. Experiments were carried out using two dosing regimes, in order to investigate whether dosing over a period of a week (7 day regimen) would increase the level of reduction in K^{trans} observed following drug administration over 24h (1 day regimen). Mice bearing PC-3 xenografts and treated with ZD4190 (100 mg/kg/dose) using either the 1 day or 7 day dosing regimen, showed highly significant reductions in tumor K^{trans} (31% and 53% respectively, $p < 0.001$ for both) when compared with vehicle treated animals (Fig. 3). Although ZD4190 reduced K^{trans} in the Calu-6 lung

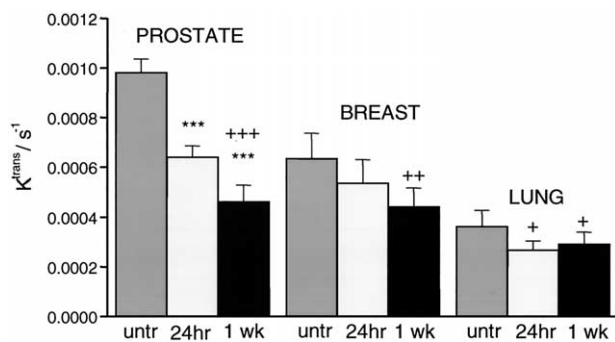


Fig. 3. The effect of dosing ZD4190 ($100 \text{ mg}\cdot\text{kg}^{-1}$) on K^{trans} for the three tumor models studied. ZD4190 was administered over a period of 24 h or one week (1 day or 7 day regimens respectively). Values are means with standard errors. Data were compared with values obtained for control tumors (vehicle treated) either by comparing mean values for K^{trans} (***) $p < 0.001$ or in the histogram analysis shown in Fig. 4 and described in the text (+ $p < 0.05$, ++ $p < 0.01$, +++ $p < 0.001$).

tumor (26% and 20% for the 24-hour and 1-week regimens, respectively) and MDA-MB-231 breast tumor (15% and 30% for the 24-hour and 1-week regimens, respectively), the reductions were not statistically significant when whole tumor data were used in the analyses. In general, there were no effects of ZD4190 on V_e , but in the prostate tumors 24-hour dosing with ZD4190 significantly reduced the mean V_e by 22% ($p = 0.01$).

3.7. Histogram analyses

The results of the cumulative histogram analyses for the 7 day dosing regime are shown in Fig. 4. Statistically significant drug-induced changes in K^{trans} were seen for the

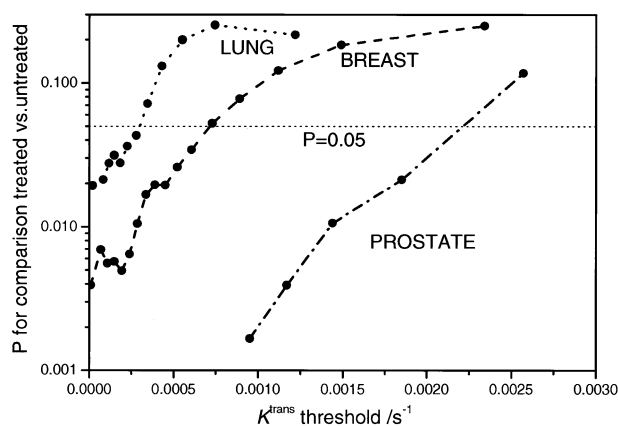


Fig. 4. A multi-thresholding histogram analysis of K^{trans} data. The analysis compares the number of voxels in treated versus control tumors over a given level of K^{trans} (top 2%, 4%, 6% . . . 100% of K^{trans} values) where the threshold level was determined by pooling all data from control or treated tumors (at a given dose level) for each tumor model studied. The data shown is for the 7 day dosing regime (see methods for details). The graph shows that at the highest threshold values of K^{trans} (2% threshold for the prostate tumor, 2–10% thresholds for the other tumors) there were no significant differences between treated and control tumors, but at intermediate and low threshold values for K^{trans} the differences became significant.

prostate tumors at thresholds below 0.0022 and 0.0019 s^{-1} for the 7 day and 1 day ZD4190 dosing regimens, respectively (data not shown in the figure). In addition, the histogram analysis enabled the detection of significant differences in K^{trans} between treated and control tumors for the lung and breast tumors. These differences were significant for the lung tumors for both dosing regimens (thresholds below 0.0003 and 0.0001 s^{-1}), but only significant for the 7 day regime in the breast tumors (thresholds below 0.0007 s^{-1}). For all the tumors studied, the voxels which were most affected were those with intermediate or low K^{trans} . None of the tumors showed a significant effect when only the highest K^{trans} voxels were included.

4. Discussion

VEGF signaling inhibitors are attractive for the treatment of diseases that are reliant on pathologic neovascularisation. With the exception of the female reproductive system and in wound healing, mature endothelia are quiescent compared to those in tumors. Since VEGF is a pivotal angiogenic growth factor, several approaches to inhibiting VEGF-signal transduction are currently being evaluated clinically for the treatment of solid tumors. These include antibodies that prevent ligand-receptor interaction by sequestering VEGF [28,29] and orally bioavailable inhibitors of VEGF-receptor tyrosine kinase activity [30]. While these strategies are anticipated to induce disease stabilization upon chronic treatment, earlier correlates of biologic activity are being sought.

This study aimed to determine preclinically whether dynamic contrast enhanced magnetic resonance imaging (DCEMRI) was appropriate for measuring effects on tumors following relatively acute treatment with the VEGF signaling inhibitor ZD4190. Nude mice, bearing human prostate (PC-3), lung (Calu-6) and breast (MDA-MB-231) tumor xenografts were dosed orally with ZD4190, using a 1 day or 7 day dosing regimen, and DCEMRI used to measure K^{trans} , the transfer constant for gadopentetate into the tumor. Reductions in K^{trans} were induced by ZD4190 treatment in each tumor model examined, which is consistent with an inhibition of VEGF signaling and a reduction in vascular permeability. Other studies have reported changes in macromolecular DCEMRI measured vascular permeability in experimental tumors treated with antibody approaches to inhibit VEGF signaling [16,22,31]. The largest reduction in K^{trans} was observed in the human prostate tumor model (PC3) following treatment over a 7 day period, although a significant reduction in K^{trans} was evident following only 2 doses of compound (0 h and 22 h; 1 day regimen). ZD4190 has been shown to inhibit the growth of these prostate, lung and breast tumor models significantly, when administered chronically [9], but unlike K^{trans} analysis, caliper measurement of tumor volume can only detect a significant response

to treatment following a sustained period of administration (typically ≥ 7 days) [9].

In Calu6 and MDA-MB-231 tumors, the reduction of K^{trans} was perhaps limited by the already low pre-treatment K^{trans} values. However multi-thresholding histogram analysis revealed significant effects on K^{trans} . Using this approach, it was possible to show that separate areas of the tumors respond differently to treatment with ZD4190. In particular, the lack of significance seen at thresholds that included only the highest values of K^{trans} suggested that both the control and treated tumors had similar numbers of voxels with high values for K^{trans} . This may represent the highly vascular tumor rim which can involve additional co-opted vessels from pre-existing host vasculature [32]. When intermediate and low levels of K^{trans} were included in the histogram analyses then significant differences were seen between treated and control tumors. The results obtained using the histogram analysis illustrate the value of a regional analysis when examining the effects of VEGF signaling inhibition using DCEMRI. Methods for dealing with the analysis of groups of K^{trans} maps are not well developed and many studies still use a manually selected ROI. Grouping together all voxels may not be desirable, since the regions with high, intermediate and low values for K^{trans} may respond very differently to VEGF signaling inhibitors. The multi-threshold analysis developed for this study was an improvement over the mean because the method gives equal weighting to each tumor voxel and was therefore not sensitive to outlying values. There is a clear need for further studies to evaluate a histogram approach to analyzing K^{trans} data from tumors.

The K^{trans} measurement combines flow, vascular density, vascular structure and vascular permeability. All of these features may be affected by ZD4190 and it is not possible to isolate permeability from flow effects. However the reduction in V_e after 24-hour dosing in the PC-3 tumor points to a reduction in permeability rather than reduced flow. Use of K^{trans} as a measure of permeability assumes that flow is not limiting and that flow is always much greater than permeability [23]. This is clearly a problem in the center of the tumors where there is necrosis. However, much of the low flow areas in the tumor center were unfittable and consequently the more vascular areas tended to dominate the measurements. In the more vascular rim the model may be giving a better approximation. Since the threshold analysis revealed a reduction in K^{trans} in two of the tumors after only two doses, this measurement may be an early predictor of response to treatment. Further experiments are required to examine dose-response relationships using the histogram analysis.

This study has shown that gadopentetate DCEMRI can be used to measure the acute effects of VEGF-signaling inhibitors. The method should be easy to apply in human tumors as part of early phase clinical trials of VEGF signaling inhibitors.

References

- [1] Folkman J. Angiogenesis research: from laboratory to clinic. *Forum Genova* 1999;9:59–62.
- [2] Ferrara N. Molecular and biological properties of vascular endothelial growth factor. *J Mol Med* 1999;77:527–43.
- [3] Pepper MS, Ferrara N, Orci L, Montesano R. Potent synergism between vascular endothelial growth factor and basic fibroblast growth factor in the induction of angiogenesis in vitro. *Biochem Biophys Res Commun* 1992;189:824–31.
- [4] Gerlowski LE, Jain RK. Microvascular permeability of normal and neoplastic tissues. *Microvasc Res* 1986;31:288–305.
- [5] Meyer M, Clauss M, Lepple-Wienhues A, Waltenberger J, Augustin HG, Ziche M, Lanz C, Buttner M, Rziha HJ, Dehio C. A novel vascular endothelial growth factor encoded by Orf virus, VEGF-E, mediates angiogenesis via signalling through VEGFR-2 (KDR) but not VEGFR-1 (Flt-1) receptor tyrosine kinases. *Embo J* 1999;18:363–74.
- [6] Gille H, Kowalski J, Li B, LeCouter J, Moffat B, Zioncheck TF, Pelletier N, Ferrara N. Analysis of biological effects and signaling properties of Flt-1 (VEGFR-1) and KDR (VEGFR-2). A reassessment using novel receptor-specific vascular endothelial growth factor mutants. *J Biol Chem* 2001;276:3222–30.
- [7] Ferrara N, Alitalo K. Clinical applications of angiogenic growth factors and their inhibitors. *Nat Med* 1999;5:1359–64.
- [8] Cross MJ, Claesson-Welsh LF. GF and VEGF function in angiogenesis: signalling pathways, biological responses, and therapeutic inhibition. *Trends Pharmacol Sci* 2001;22:201–7.
- [9] Wedge SR, Ogilvie DJ, Dukes M, Kendrew J, Curwen JO, Hennequin LF, Thomas AP, Stokes ES, Curry B, Richmond GH, Wadsworth PF. ZD4190: an orally active inhibitor of vascular endothelial growth factor signaling with broad-spectrum antitumor efficacy. *Cancer Res* 2000;60:970–5.
- [10] Herbst RS, Lee AT, Tran HT, Abbruzzese JL. Clinical studies of angiogenesis inhibitors: the University of Texas MD Anderson Center Trial of Human Endostatin. *Curr Oncol Rep* 2001;3:131–40.
- [11] Braybrooke JP, O'Byrne KJ, Propper DJ, Blann A, Saunders M, Dobbs N, Han C, Woodhull J, Mitchell K, Crew J, Smith K, Stephens R, Ganesan TS, Talbot DC, Harris AL. A phase II study of razoxane, an antiangiogenic topoisomerase II inhibitor, in renal cell cancer with assessment of potential surrogate markers of angiogenesis. *Clin Cancer Res* 2000;6:4697–704.
- [12] Hawighorst H, Knapstein PG, Weikel W, Knopp MV, Zuna I, Knof A, Brix G, Schaeffer U, Wilkens C, Schoenberg SO, Essig M, Vaupel P, van Kaick G. Angiogenesis of uterine cervical carcinoma: characterization by pharmacokinetic magnetic resonance parameters and histological microvessel density with correlation to lymphatic involvement. *Cancer Res* 1997;57:4777–86.
- [13] Eskey CJ, Koretsky AP, Domach MM, Jain RK. 2H-nuclear magnetic resonance imaging of tumor blood flow: spatial, and temporal heterogeneity in a tissue-isolated mammary adenocarcinoma. *Cancer Res* 1992;52:6010–9.
- [14] Zhu XP, Li KL, Kamaly-Asl ID, Checkley DR, Tessier JJ, Waterton JC, Jackson A. Quantification of endothelial permeability, leakage space, and blood volume in brain tumors using combined T1 and T2* contrast-enhanced dynamic MR imaging. *J Magn Reson Imaging* 2000;11:575–85.
- [15] Furman-Haran E, Grobgeld D, Degani H. Dynamic contrast-enhanced imaging and analysis at high spatial resolution of MCF7 human breast tumors. *J Magn Reson Imaging* 1997;128:161–71.
- [16] Pham CD, Roberts TP, van Bruggen N, Melnyk O, Mann J, Ferrara N, Cohen RL, Brasch RC. Magnetic resonance imaging detects suppression of tumor vascular permeability after administration of antibody to vascular endothelial growth factor. *Cancer Invest* 1998;16:225–30.

- [17] Parker GJ, Suckling J, Tanner SF, Padhani AR, Revell PB, Husband JE, Leach MO. Probing tumor microvascularity by measurement, analysis and display of contrast agent uptake kinetics. *J Magn Reson Imaging* 1997;7:564–74.
- [18] Tofts PS, Berkowitz B, Schnall MD. Quantitative analysis of dynamic Gd-DTPA enhancement in breast tumors using a permeability model. *Magn Reson Med* 1995;33:564–8.
- [19] Degani H, Gusic V, Weinstein D, Fields S, Strano S. Mapping pathophysiological features of breast tumors by MRI at high spatial resolution. *Nat Med* 1997;3:780–2.
- [20] Furman-Haran E, Margalit R, Grobgeld D, Degani H. Dynamic contrast-enhanced magnetic resonance imaging reveals stress-induced angiogenesis in MCF7 human breast tumors. *Proc Natl Acad Sci USA* 1996;93:6247–51.
- [21] Brasch R, Turetschek K. MRI characterization of tumors, and grading angiogenesis using macromolecular contrast media: status report. *Eur J Radiol* 2000;34:148–55.
- [22] Gossman A, Helbich TH, Mesiano S, Shames DM, Wendland MF, Roberts TP, Ferrara N, Jaffe RB, Brasch RC. Magnetic resonance imaging in an experimental model of human ovarian cancer demonstrating altered microvascular permeability after inhibition of vascular endothelial growth factor. *Am J Obstet Gynecol* 2000;183:956–63.
- [23] Tofts PS, Brix G, Buckley DL, Evelhoch JL, Henderson E, Knopp MV, Larsson HB, Lee TY, Mayr NA, Parker GJ, Port RE, Taylor J, Weisskoff RM. Estimating kinetic parameters from dynamic contrast-enhanced T(1)-weighted MRI of a diffusible tracer: standardized quantities and symbols. *J Magn Reson Imaging* 1999;10:223–32.
- [24] Tofts PS, Kermode AG. Measurement of the blood-brain barrier permeability and leakage space using dynamic MR imaging. 1. Fundamental concepts. *Magn Reson Med* 1991;17:357–67.
- [25] Larsson HB, Stubgaard M, Frederiksen JL, Jensen M, Henriksen O, Paulson OB. Quantitation of blood-brain barrier defect by magnetic resonance imaging and gadolinium-DTPA in patients with multiple sclerosis and brain tumors. *Magn Reson Med* 1990;16:117–31.
- [26] Harkness JE, Wagner JE. The biology and medicine of rabbits and rodents. Williams and Wilkins, 1995.
- [27] Siegel S, Castellan NJ. Nonparametric statistics for behavioural sciences. McGraw-Hill, 1988.
- [28] Johnson DH, DeVore R, Kabbinar F, Herbst R, Holmgren E, Novotny W. Carboplatin (C) + paclitaxel (T) + rhuMab-VEGF (AVF) may prolong survival in advanced non-squamous lung cancer. *Proc Am Assoc Cancer Res* 2001;12:1256 (Abstract).
- [29] Jayson GC, Mulatero C, Ranson M, Zweit J, Hastings D, Julyan P, Lawrance J, McGown A, Jackson A, Haroon H, Hakansson L, Wagstaff J, Groenewegen G, Lehmann F, Levitt D, Tang T, Zweirzina H. Anti-VEGF antibody HuMV833: an EORTC biological treatment development group phase I toxicity, pharmacokinetic, and pharmacodynamic study. *Proc Am Assoc Cancer Res* 2001;12:14 (Abstract).
- [30] Basser R, Hurwitz H, Barge A, Davis I, DeBoer R, Holden S, McArthur G, McKinley M, Nairn K, Persky M, Rischin D, Rosenthal M, Swaisland H, Eckhardt G. Phase I pharmacokinetic, and biological study of the angiogenesis inhibitor, ZD6474, in patients with solid tumors. *Proc Am Assoc Cancer Res* 2001;12:396 (Abstract).
- [31] Brasch R, Pham C, Shames D, Roberts T, van Dijke K, van Bruggen N, Mann J, Ostrowitzki S, Melnyk O. Assessing tumor angiogenesis using macromolecular MR imaging contrast media. *J Magn Reson Imaging* 1997;7:68–74.
- [32] Thompson WD, Shiach KJ, Fraser RA, McIntosh LC, Simpson JG. Tumours acquire their vasculature by vessel incorporation, not vessel ingrowth. *J Pathol* 1987;151(4):323–32.